Thermochimica Acta, 44 (1981) 171—187
Elsevier Scientific Publishing Company, Amsterdam — Printed in Belgium

THERMAL AND MOSSBAUER STUDIES OF IRON-CONTAINING HYDROUS SILICATES. III. CRONSTEDTITE

K.J.D. MACKENZIE and R.M. BEREZOWSKI

Chemistry Division, Department of Scientific and Industrial Research, Private Bag, Petone (New Zealand)

(Received 25 August 1980)

ABSTRACT

The thermal transformations of a disordered polycrystalline cronstedtite have been studied in both oxidising and reducing atmospheres by thermal analysis, X-ray powder diffraction, IR and Mossbauer spectroscopy. After low-temperature loss of surface adsorbed water, hydroxyl water is lost by internal oxidation of Fe^{2+} to Fe^{3+} under both oxidising and reducing conditions. Removal of further hydroxyl water from this oxycronstedtite results in the progressive formation of an intermediate phase containing both iron and silicon in intimate association; when formed under oxidising conditions this intermediate adopts a hexagonal structure which subsequently transforms to hematite Reducing atmospheres favour the formation of a cubic intermediate which subsequently transforms to an olivine, and, on further reduction, to iron metal and cristobalite.

INTRODUCTION

Cronstedtite is a hydrous iron silicate named after the Swedish mineralogist and chemist A.F. Cronstedt. Structurally it is a member of the septechlorite family and is related to ideal amesite, $(Si_2Al_2)(Mg_4Al_2)O_{10}(OH)_8$, by complete replacement of Mg and Al by Fe^{2+} and Fe^{3+}, resulting in an ideal formula of $(Si_2Fe^{3+}_2)(Fe^{2+}_4Fe^{3+}_2)O_{10}(OH)_8$. Its structural relationship to serpentine is therefore apparent, since ideal amesite can be considered as being derived by the partial replacement of Mg by Al in serpentine $[Si_4Mg_6O_{10}(OH)_8]$.

Published room-temperature Mossbauer spectra of unheated cronstedtite [1,2] show broad, poorly-resolved peaks which have been interpreted in terms of the above structure. Several polymorphs of cronstedtite have been identified, which differ in their stacking sequence [3]. When heated in air, all polymorphs oxidise to the ferric form at ~275°C with a slight contraction of the lattice parameter, but remain otherwise structurally unchanged [4]. By about 720°C a new phase appears, the structure of which depends on the stacking sequence of the starting material; polymorphs with a one-layer sequence adopt a cubic spinel structure whereas those with two-layer and six-layer stacking form a hexagonal ferrite structure [5]. The spinel and ferrite phases are considered to contain both Si and Fe, and occur initially in small zones which increase in number with increasing temperature until they

0040-6031/81/0000—0000/$02.50

occupy the entire volume of the crystal [5]. Above ~750°C the cubic or hexagonal phase decomposes to hematite (α-Fe_2O_3), and, at higher temperatures, cristobalite appears [4]. Polymorphs of cronstedtite with a three-layer stacking sequence lose their structure on thermal oxidation, and do not form a series of crystalline intermediates, possibly due to an unsuitable cation-oxygen configuration occurring in that stacking sequence [5].

Another view of the thermal decomposition of cronstedtite is taken by Babcan [6] who states that the mineral decomposes to its primary oxides which at 500°C give the spinel γ-Fe_2O_3 in oxidising conditions, magnetite (Fe_3O_4) in inert atmospheres and metallic Fe in hydrogen.

In the present study of the thermal behaviour of cronstedtites, thermal analysis, X-ray diffraction, IR and Mossbauer spectroscopy were used to gain information about the intermediate stages in the decomposition under both oxidising and reducing conditions. The suggested formation of an Fe—Si spinel intermediate [5] is of considerable interest, since if formed it should bear some relationship to the Al—Si spinel in the thermal decomposition of kaolinite.

EXPERIMENTAL

(a) Material

The cronstedtite studied here was from sample B13823 of the mineral collection, Smithsonian Institution, Washington, kindly made available by Dr. P.E. Desautels. This material, from Kisbanya, Rumania consisted of small black crystals which could be hand-picked from the groundmass. X-Ray diffraction indicated monomineralic well-crystallised cronstedtite. The chemical analysis of the black material is shown in Table 1, which includes for comparison analyses of another sample from the same location and of two samples from Pribram, C.S.S.R., (the locality of the type material). The analyses show that the present cronstedtite is similar to those studied by other workers, and is in reasonable agreement with the ideal cronstedtite composition. Calculations of the structural formulae based on 18 oxygen atoms per unit are also given in Table 1, which shows reasonable agreement between all four cronstedtites and the ideal formula. Arc-spectral analysis of sample B13823 shows the only significant trace impurity to be boron, present at a concentration of ~500 ppm.

(b) Methods

Since only a small amount of the black crystalline material was available, the serial heating method was used, as previously described [8]. Firings were made in air and 5%/95% H_2/N_2 mixture, the sampling temperatures being chosen from the DTA traces obtained under the appropriate atmosphere. The TG, X-ray, IR and Mossbauer techniques have been described elsewhere [8].

TABLE 1

Chemical analyses and unit cell contents of cronstedtites, calculated on the basis of 18 (O+ (OH))

Component	1	2	3	4
SiO_2	14.27	16.42	20.81	22.21
Al_2O_3	1.05	0.90	1.54	
TiO_2	0.05			
Fe_2O_3	33 70	29.72	33.12	37.49
FeO	39.22	41.86	29.58	25.28
MnO				1.20
MgO	0.64		5.40	5.23
CaO	0.06	1.32		
Na_2O	0.48			
K_2O	<0.01			
$H_2O(+)$	10.36	10.17	8.28	8.27
$H_2O(-)$			0.63	
Total	99.83	100 39	99.36	99.68

Column 1. Present sample, Kisbanya, Rumania, B. 13823, Smithsonian collection. Analyst A.D. Cody.
Column 2. Cronstedtite, Kisbanya, Rumania, after Hendricks [7]. Analyst B. Gossner.
Column 3. Cronstedtite, Pribram, after Babcan [6].
Column 4. Type material, Pribram. Analyst E. Ludwig (1891).

		Unit cell contents									
		1		2		3		4		5	
Si	Tetra-hedral	1.87	4.0	2.14	4.0	2.63	4.0	2.77	4.0	2.0	4.0
Al		0.16		0.14		0.23					
Fe^{3+}		1.97		1.72		1.14		1.23		2.0	
Fe^{3+}	Octa-hedral	1.34	5.95	1.17	5.89	2.02	6.17	2.27	6.04	2.0	6.0
Fe^{2+}		4.29		4.53		3.13		2.63		4.0	
Ca				0.19							
Mg		0.13				1.02		0.98			
Na		0.19									
Mn								0.16			
OH		9.05		8.83		7.01		6.88		8.0	

Column 1. Present sample, B13823, Kisbanya.
Column 2. Kisbanya, after Hendricks [7].
Column 3. Pribram, after Babcan [6].
Column 4. Pribram, type material.
Column 5. Ideal cronstedtite.

RESULTS AND DISCUSSION

(a) Thermal analysis

The DTA and TG traces are shown in Fig. 1.
The DTA traces are characterised by two groups of endotherms, the

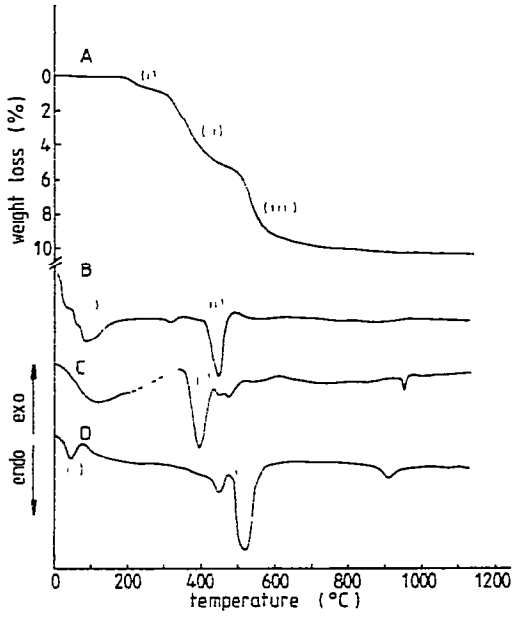

Fig. 1. TG and DTA curves of cronstedtite, sample B13823, Kisbanya. Heating rate 10°C min^{-1}. A, TG curve in oxygen-free nitrogen; B, DTA curve in oxygen-free nitrogen; C, DTA curve in hydrogen/nitrogen, D, DTA curve in air. Dashed portion of curve C indicates region where background curve was subtracted to eliminate noise due to adsorption of H_2 by the platinel thermocouples.

lower-temperature feature, designated (i), resulting from the loss of water adsorbed on to the surface of the powdered sample. The second endothermic feature (ii), at 400—530°C corresponds with the loss of hydroxyl water and is the most prominent feature of previously published cronstedtite DTA traces [9]. The shape and temperature of the dehydroxylation endotherm (ii) are sensitive to the reaction atmosphere, a result similar to those reported for other iron-containing serpentine varieties in which inhibition or facilitation of iron oxidation causes wide variations in the shape of the dehydroxylation endotherm [9]. In the present case more than one endotherm was recorded in the dehydroxylation region, especially under oxidising conditions. The absence of recrystallisation exotherms such as observed in iron-poor serpentines is in agreement with previous work [9] and has been attributed to the fact that recrystallisation in the iron-rich varieties occurs simultaneously with dehydroxylation, the thermal effect of the former being masked by the latter. The temperature of the dehydroxylation endotherm (ii) depends on the oxygen partial pressure of the reaction atmosphere; under reducing conditions it is lowered to 400°C [coinciding with the temperature at which reduction sets in — see Sect. (d)], whereas under oxidising conditions the major feature occurs at ~520°C, coinciding with the temperature at which oxidation of the octahedral Fe^{2+} is complete. The dehydroxylation temperature in nitrogen is intermediate between these two extremes.

The origin of the small endotherms at 900—950°C in H_2/N_2 and air is not clear; these peaks do not correspond with any phase change detectable by XRD or Mossbauer spectroscopy.

The TG curve, obtained under oxygen-free nitrogen (Fig. 1A) shows a weight loss occurring in at least three stages. The first loss, of ~0.7% (i), is associated with the DTA endotherm (i), and appears to be due to the loss of mechanically-held water. The second loss, of ~4.6% [Fig. 1A, region (ii)], occurs in the temperature range of oxidation of lattice Fe^{2+} to Fe^{3+} [Sect. (d)]. Although Mossbauer spectroscopy was not carried out on samples heated in nitrogen, samples heated under more reducing conditions were progressively internally oxidised up to the onset of reduction at 430°C [Sect. (d)]. It is therefore not unreasonable to expect a similar process to occur in inert atmospheres over a similar temperature range.

The simultaneous oxidation and dehydroxylation of hydrous silicates containing Fe^{2+} can be represented [10a, b] in air as

$$4\ Fe^{2+} + 4\ OH^- + O_2 \rightarrow 4\ Fe^{3+} + 4\ O^{2-} + 2\ H_2O \qquad (1)$$

Although this equation is considered to define the principal reaction of hydrous silicates in air [10a, b] two other side-reactions are also possible

$$2\ Fe^{2+} + O_2 \rightarrow 4\ Fe^{3+} + 2\ O^{2-} \qquad (2)$$

and

$$2\ OH^- \rightarrow O^{2-} + H_2O \qquad (3)$$

Reaction (2) probably occurs at the mineral surfaces when all the available hydroxyls have been used up, while reaction (3) occurs at sufficiently elevated temperatures in all hydroxylated minerals irrespective of the redox processes occurring [10a, b]. Where oxygen is not available to the sample, oxidation of Fe^{2+} and dehydroxylation occur by dehydrogenation [11]

$$Fe^{2+} + OH^- \rightarrow Fe^{3+} + O^{2-} + H\cdot \qquad (4)$$

At the surface, the H· either reacts with any available oxygen to form water, or, in vacuum conditions, evolves as H_2. Where some oxygen is available to form water, eqn. (4) has the same practical consequences as eqn. (1), in that 2 moles Fe^{2+} produce 1 mole of water. From the chemical analysis of the present mineral (Table 1), oxidation of the total Fe^{2+} content can be calculated to produce a weight of water equal to 4.8% of the total mineral weight, in good agreement with the 4.6% weight loss observed in stage (ii) of the TG curve, up to ~450°C (Fig. 1A). On the other hand, oxidation of the total available Fe^{2+} according to eqn. (4) would result in a weight loss of 0.54%. It is therefore clear that this cannot represent the weight-loss mechanism over the temperature range of Fe^{2+} oxidation. Above 450°C the available Fe^{2+} is exhausted under inert or oxidising conditions and the elimination of the remaining hydroxyl water must then proceed according to eqn. (3). This corresponds to stage (iii) of the weight-loss curve (~4.0% up to 600°C).

The mechanism by which the first stage of hydroxyl elimination proceeds [Fig. 1A, region (ii)], according to eqn. (4), involves the transfer of both protons and electrons from the bulk of the crystal to the surface [10a, b], the nett result being the same as if OH^- and Fe^{2+} ions in the bulk had exchanged with O^{2-} and Fe^{3+} at the surface. Such a process can occur with little or no disruption of the crystal structure. On the other hand, the second

stage of dehydroxylation [region (iii)], according to eqn. (3), can have rather more disruptive effects in minerals related to cronstedtite; in kaolinite ($Al_4Si_4O_{10}(OH)_8$) the product of complete dehydroxylation is largely X-ray amorphous, while in serpentine ($Mg_6Si_4O_{10}(OH)_8$) complete dehydroxylation is accompanied by an immediate recrystallisation of magnesium silicates [12]. X-Ray studies of the present sample [Sect. (b)] show that in the temperature range corresponding to the weight loss of region (ii), the cronstedtite structure persists, whereas during the weight loss in region (iii) (>420°C) the structure is progressively replaced by new iron-containing phases. (The X-ray results were obtained for both oxidised and reduced samples but are likely to apply also to inert conditions.) Thus, all the evidence is consistent with the suggestion that the first major weight loss is due to dehydroxylation by a mechanism involving oxidation of Fe^{2+}, the presence of the necessary oxygen presumably arising through imperfect purging of the thermobalance. The second hydroxyl weight loss [region (iii)] sets in when all the Fe^{2+} has been exhausted, and is accompanied by the progressive formation of new phases.

(b) X-Ray diffraction

Since previous single-crystal studies of cronstedtites have indicated that the stacking sequence of the starting material can influence the structure of the decomposition products [5], it was of interest to ascertain the predominant stacking pattern of the sample used here. For this purpose, small crystals were hand-picked for examination in a precession camera. All the larger crystals proved to be extensively intergrown, but precession photographs of finely crushed fragments (~0.2 mm) showed evidence of sufficient short-range order for some symmetry and cell dimensions to be determined. Nevertheless, even in the small crystals, long-range stacking disorder occurs, as indicated by streaking in the photographs. Measurements made on the ordered portion of one of the small fragments appear to show hexagonal symmetry, with a basal spacing of 7.07 Å. In view of the overall stacking disorder and crystal intergrowth in the present sample, it is impossible to tell whether this one-layer region is typical of the bulk sample. A similar problem was encountered by Hendricks [7] who found that cronstedtite crystals from the same locality gave photographs which were too distorted to permit determination of symmetry. The effect of heating such a disordered material cannot readily be predicted by analogy with results previously reported for single crystals of unique stacking order [5] since it is quite possible that several different stacking sequences could exist in the bulk of the same crystal. The powder pattern of the crushed bulk sample agreed reasonably well with the *d*-values calculated for a hexagonal unit cell with Steadman and Nuttall's parameters $a = 5.49$ Å, $b = 7.085$ Å [3], but was equally well fitted by JCPDS card No. 17-470 which is indexed on a monoclinic cell of space group *Cm*. This space group is the only one capable of indexing all the observed reflections of all eight known polymorphs. Some of the lines in the observed powder pattern which could not be accounted for in terms of hexagonal reflections were present in the monoclinic listing, sug-

gesting that the bulk material is not solely of the hexagonal variety.

On heating, the cronstedtite pattern persists to 510°C in air (430°C in H_2/N_2), but changes are observed in both the position and intensity of the major lines. The observed changes in the *d*-spacings of the basal reflections suggest that during the initial loss of mechanically-held water the lattice expands slightly in the *c*-direction, but at 200—300°C in air it contracts due to oxidation. Different behaviour is observed in H_2/N_2, in which the lattice appears to expand continuously throughout the dehydroxylation process. Under both oxidising and reducing conditions, these changes are accompanied by a progressive loss of intensity of all the cronstedtite peaks. The changes in the *c*-parameter are very similar to those observed in single

TABLE 2

X-Ray data for intermediate phases from fired cronstedtite, compared with those of possible related phases (*d*-values in Å. Major cronstedtite lines at 7.08, 3 52, 2 78 and 2.36 Å omitted)

A. Fired in air

Cronstedtite		Hexagonal ferrite *	η-Fe_2O_3 **	α-Fe_2O_3
410°C	510°C			
	6 56	6.72		
5.98	6.03		6.01	
4 35	4 33	4.39	4 36	
3.59	3.59	3.59	3 60	3.67
2.99	2.99	2.98	3.0	
2.96				
2.74	2.74	2.78	2.74	
2.69	2.69	2.69		2 69
2.66	2 67	2 67		
	2.53	2.53		2.514

B. Fired in H_2/N_2

Cronstedtite		Fe—Si spinnel ***	FeO (wustite)	Fe_3O_4 (magnetite)	γ-Fe_2O_3 (maghemite)
430°C	530°C				
2.98 (b)	2.98	2.95		2 970	2.95
2.65	2.65				
2.52	2.52	2.51	2.475	2.532	2.514
	2.43			2.425	
2.40 (b)	2.40	2.40			
2.08 (b)	2.08 (b)	2.08	2.145	2.100	2 086
1.48 (b)	1.48 (b)	1.47	1.515	1.485	1.44

* Calculated from data of Steadman and Toy [5], with a = 8 78 Å, c = 14.35 Å
** Data from Walter-Levy and Quemeneur [13]
*** Calculated from data of Steadman and Toy [5], with a = 8.33 Å.
All reflections not related to the observed pattern omitted.
b = broad peak.

crystals by Steadman and Toy [5] during the formation of ferric cronstedtite.

Under oxidising conditions, the loss of the cronstedtite reflections is accompanied by the appearance of several new weak, broad peaks which appear at 410°C and persist to at least 510°C. Table 2 compares these new *d*-spacings with those calculated from the lattice parameters given by Steadman and Toy [5] for their cubic spinel and hexagonal phases.

No correspondence is seen between the present lines and those of the cubic spinel, although some matching is found with the calculated hexagonal ferrite pattern (Table 2). The fit is less perfect than might be supposed from Table 2, however, which only shows the observed lines additional to those of the original cronstedtite, and from which the calculated lines not observed in the powder pattern have been omitted. One of the most significant absences from the observed pattern is the calculated 001 spacing at 14.35 Å, arising from the fact that Steadman and Toy's hexagonal ferrite is a two-layer structure [5]. It is interesting that a very weak 14.4 Å reflection was noted in the pattern of the unheated material; heating at 200°C in both air and H_2/N_2 intensifies this peak slightly but it disappears >200°C and is therefore unlikely to be associated with the higher-temperature ferrite.

Another phase with an X-ray pattern similar in some respects to that of heated cronstedtite was reported as an intermediate in the thermal decomposition of basic ferric sulphates [13] and is described as a transition form of Fe_2O_3, designated η-Fe_2O_3. Although it has apparently not been structurally investigated, a number of its peaks correspond with those of the hexagonal ferrite of Steadman and Toy [5], suggesting a degree of structural similarity (Table 2), even though by virtue of its origin, η-Fe_2O_3 cannot contain silicon as a structural requirement. The transition phase of this study in air is probably best described as a hexagonal phase in which silicon is a possible but not essential component. On heating to higher temperatures in air, the ferrite peaks abruptly disappear, with the exception of those which gradually develop into α-Fe_2O_3 (Table 2). At still higher temperatures the silica expelled during the formation of hematite recrystallises as cristobalite. A schematic view of the reaction sequence is shown in Fig. 2.

Under reducing conditions the disappearance of the cronstedtite peaks at ~400°C is accompanied by the appearance of new peaks (Table 2) unlike those of the hexagonal ferrite but having several spacings in common with the pattern calculated from the lattice parameter of Steadman and Toy's Fe—Si spinel [5]. Table 2 also shows the similarity between the new phase and other cubic iron oxide phases, but again, lines not observed in the heated cronstedtite are omitted. On this basis, γ-Fe_2O_3 must be ruled out since its pattern contains more lines than are observed in heated cronstedtite, and similarly FeO can probably be ruled out also since its pattern contains fewer lines than were observed. Magnetite, Fe_3O_4, accounts more satisfactorily for the number of peaks observed, but its *d*-values are not in good agreement with those of heated cronstedtite. Furthermore, the diagnostic six-line Mossbauer spectrum of magnetite is absent in these samples [Sect. (d)]. The cubic phase therefore seems to be similar to the Fe—Si spinel of Steadman and Toy. Some indirect evidence for the presence of silicon in this phase is pro-

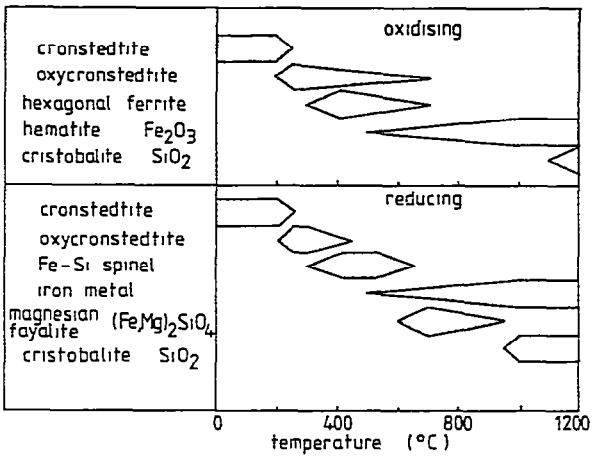

Fig. 2. Schematic representation of the phases formed from cronstedtite as a function of temperature under oxidising and reducing conditions.

vided by its smooth transformation to olivine on further reduction; the apparent structural continuity of this process argues the presence of silicon in the precursor phase. At higher temperatures, further reduction to iron metal occurs with the expulsion of silica which eventually recrystallises as cristobalite. The reaction sequence is shown schematically in Fig. 2.

The unexpected result emerging from the X-ray results is that oxidising conditions favour the formation of a probable hexagonal intermediate phase whereas reducing conditions favour a cubic intermediate. According to Steadman and Toy [5], both structures are formed by a two-stage process, the first stage involving rotation of the tetrahedral units of cronstedtite through 30° about the [001] direction, forming a close-packed oxygen structure. The second stage involves the re-distribution of cations within this close-packed oxygen framework. The pattern of cation distribution determines the layer sequence of the new phase and hence whether it assumes a spinel or hexagonal structure [5]; the energetically favourable cation movements are pre-determined by the stacking order of the starting material, thereby explaining the pre-disposition of some polymorphs to form spinel intermediates and others to form hexagonal structures [5]. The temperature range in which this cation re-distribution occurs (~400—550°C) also coincides with the onset of significant Fe^{3+} reduction in H_2/N_2 [Sect. (d)], which, by changing the valence, size and site preference characteristics of these ions will also alter the energetics of their lattice re-distribution. The influence of iron valency and size on crystal structure is illustrated by the oxides Fe_2O_3 and FeO; in the former, Fe(III) adopts a hexagonal structure in its most stable oxide (hematite) whereas the preferred structure for Fe(II) oxide is cubic. These preferences would be predicted from cation interchange enthalpies measured for spinel systems [14], in which in close-packed oxygen arrays the preference of Fe^{3+} is for tetrahedral sites whereas Fe^{2+} shows a slight octahedral site preference [14]. In the hexagonal corundum structure adopted by hematite the Fe^{3+} ions are coordinated in distorted

tetrahedra, whereas the cation coordination in cubic FeO is octahedral. The formation of hexagonal or cubic intermediate structures in heated polycrystalline cronstedtite appears to be determined by similar considerations.

(c) Infrared spectroscopy

Typical IR spectra of heated and unheated cronstedtite are shown in Fig. 3. The spectrum of unheated cronstedtite (Fig. 3a) is similar to published spectra of samples from other localities [15]. The hydroxyl stretching bands at 3200—3400 cm^{-1} are by comparison with related serpentine minerals broadened and displaced to lower frequencies, similar to the effect induced in some amesites by random substitution of tetrahedral Si [16a, b]. The present hydroxyl stretching frequencies are lower than those of amesite, due to the increased octahedral iron content which affects the hydroxyl stretching frequencies of trioctahedral chlorites in this way [17]. Substitution of tetrahedral Fe^{3+} for Si increases the (Si, Fe)—O distance and the ionic character of the bond [18], thus displacing the principal Si—O stretching band to ~935 cm^{-1}. Another Si—O band occurs in trioctahedral minerals at 668—680 cm^{-1}, the higher frequency corresponding to the greater degree of Si substitution. The cronstedtite band at 680 cm^{-1} can probably be identified with this vibration. The weak band at 445 cm^{-1} is probably due to the

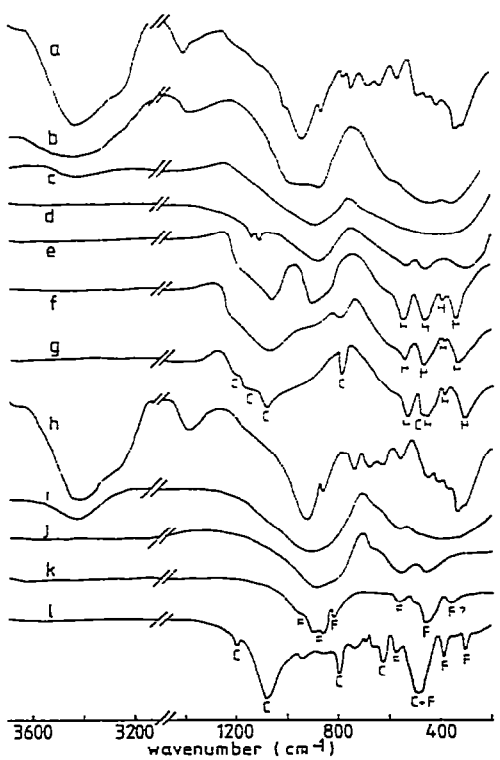

Fig. 3. Typical IR spectra of heated and unheated cronstedtite. Curves a—g heated in air. Curves h—l heated in hydrogen/nitrogen. a, Unheated (and 200°C); b, 320°C; c, 410°C; d, 510°C; e, 700°C; f, 1000°C; g, 1200°C, h, 200°C; i, 430°C; j, 530°C; k, 700°C; l, 1000°C. H = Hematite, F = fayalite, C = cristobalite.

Si—O bending mode which occurs in all these minerals at 430—460 cm^{-1}. Other bands in unheated cronstedtite can be identified by analogy with related minerals. Thus, the feature at 860 cm^{-1} could be due to an octahedral HO———Fe^{3+} vibration while the bands at 560, 485 and 420 cm^{-1} are probably due to octahedral Fe^{3+}—O—Si and Fe^{2+}—O—Si vibrations [18]. The band at 640 cm^{-1} can be identified with a peak common to natural 7 Å chlorites of high iron content [17] while the band at 740 cm^{-1} probably arises from a hydroxyl vibration coupled with octahedral Fe^{3+} [18]. This band has been said to be diagnostic for 14 Å chlorites [17] but examination of the spectra on which this suggestion is based [19] shows a similar but less-well-defined feature in the analogous 7 Å chlorites. The lower-frequency bands at 340 and 320 cm^{-1} are due to mixed vibrations involving the Si—O network, the octahedral cations and probably the hydroxyl groups [17].

On heating to 200°C in oxidising or reducing conditions, the hydroxyl stretching bands at 3200—3400 cm^{-1} are slightly broadened but the other features are unchanged. However, heating above this temperature produces drastic changes in the spectra (Fig. 3, curves b and i), including the loss of of the hydroxyl peaks and of the features between 400 and 800 cm^{-1}. By ~500°C, new broad features have begun to develop (Fig. 3, curves d and j) which bear resemblances to the spectrum of the spinel Fe_2SiO_4 [20] (Table 3). By this stage, differences between the spectra of oxidised and reduced samples have become apparent; below 800 cm^{-1} the oxidised sample shows the three broad bands of hematite, into which it eventually develops, while the reduced sample shows only two well-defined bands in this region. Comparisons between the heated cronstedtite spectra and those of related phases are shown in Table 3, from which it is seen that the reduced sample spectrum is more like those of the spinels magnetite and maghemite [21] which absorb in two general regions (~400 and 600 cm^{-1}) although maghemite exhibits considerable fine structure [21] which is absent from the present spectrum. Table 3 shows that the oxidised sample spectrum resem-

TABLE 3

Infrared bands of cronstedtite heated under oxidising and reducing conditions and of related phases

Cronstedtite, 520°C		α-Fe_2O_3 *	Fe_3O_4 *	Fe_2SiO_4 **
in air (cm^{-1})	in H_2/N_2 (cm^{-1})	(hematite)	(magnetite)	(spinel)
300		355		340
460	460	465	390 (b)	
530	570	550	580 (b)	503
	680 (sh)			630 (sh)
	780 (sh)			
880 (b)	880 (b)			835 (b)
	1000 (sh)			1020 (sh)

* Taken from ref. 21.
** Taken from ref. 20.
b = broad band; sh = shoulder.

bles that of hematite with the addition of an Si—O vibration whose frequency is characteristic of a lattice in intimate association with iron atoms rather than the higher frequencies typical of pure silica phases. The Si—O frequency in the reduced sample is also lower than in pure silica phases, and resembles the spectrum of Fe_2SiO_4 spinel.

On further heating in air, hematite becomes more prominent and at the highest temperatures, cristobalite also appears (Fig. 3, curves f and g). At 700°C, the system passes through an interesting stage of silica separation where pure silica and iron silicate-type Si—O bands coexist in the sample (Fig. 3, curve e); the separation of discrete silica units possibly starts at even lower temperatures as indicated by the small double peak between 1100 and 1200 cm^{-1} (Fig. 3, curve d).

Under reducing conditions, heating beyond the cubic stage results in the appearance of peaks corresponding to fayalite which develop smoothly from the principal absorptions of the cubic phase (Fig. 3, curve k). At higher temperatures a well-defined cristobalite spectrum also appears.

In summary, the IR spectra show that at >200°C the hydroxyl bands of cronstedtite are lost and a featureless spectrum develops, in which, however, the silica and iron components remain in association. At ~500°C in air a hematite precursor becomes apparent, in which, however, silica is retained in close association, becoming progressively expelled only at higher temperatures. At ~500°C under reducing conditions, a fayalite precursor becomes apparent, with characteristics similar to those of a ferrous silicate spinel. The silica remains in close association with iron during the development of fayalite, separating as cristobalite only as a consequence of further reduction of the fayalite at higher temperatures. Thus, the IR results confirm and augment the conclusions drawn from the X-ray studies.

(d) Mossbauer spectroscopy

Typical room-temperature Mossbauer spectra of cronstedtite heated in air and H_2/N_2 are shown in Figs. 4 and 5, respectively.

Comparison of the spectrum of unheated cronstedtite (Fig. 4A) with the two previously published spectra [1,2] shows closer similarities to that of Weaver et al. [1] for a specimen of undescribed origin than to that of Taylor et al. [2] whose sample came from the same locality as the present sample, but from a differently numbered specimen. Neither of the previously published spectra were computer-fitted although both were described in terms of one Fe^{2+} and two Fe^{3+} doublets, on the basis of structural considerations. The present spectrum was satisfactorily computer-fitted in this way, which, however, led to rather wide Fe^{2+} peaks (0.59 mm s^{-1}). All attempts to include an additional Fe^{2+} doublet resulted in poorer fits, and it was concluded that the spectrum contains only one ferrous doublet. The isomer shifts (I.S.) and quadrupole splittings (Q.S.) are shown in Table 4.

The ferric doublets with the smaller I.S. and Q.S. values are typical of tetrahedral Fe^{3+}, having similar parameters to tetrahedral Fe^{3+} reported by Rozenson et al. [22] for some closely-related serpentine minerals (I.S. = 0.21, Q.S. = 0.40—0.42 mm s^{-1}). The significantly greater area of these peaks

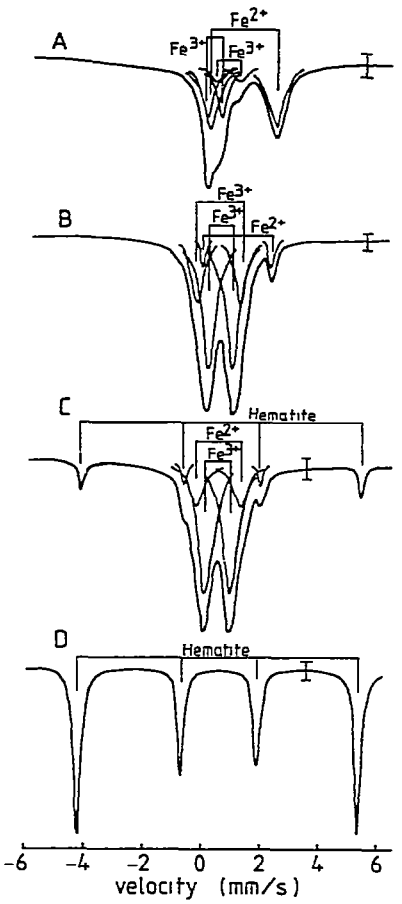

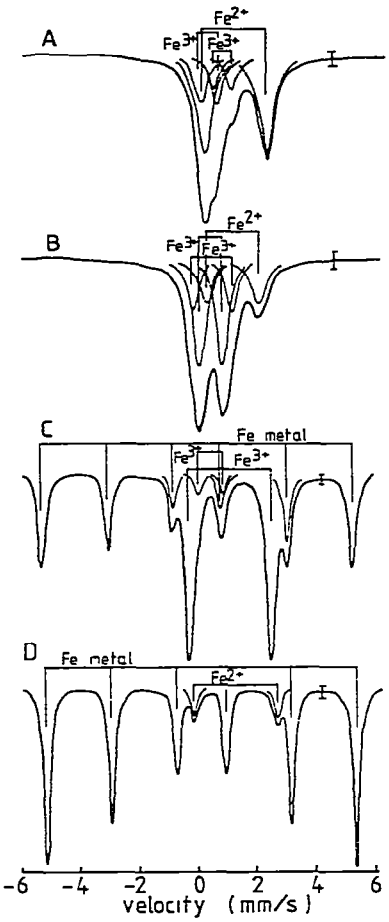

Fig. 4. Typical room-temperature Mossbauer spectra of cronstedtite unheated and heated in air. A, Unheated and 200°C; B, 320—410°C, C, 510—700°C; D, 1000—1200°C

Fig. 5. Typical room-temperature Mossbauer spectra of cronstedtite heated in hydrogen/nitrogen. A, 200°C; B, 430—530°C; C, 700°C, D, 1000—1200°C.

is also consistent with the calculated structural formula (Table 1) in which the proportion of tetrahedral Fe^{3+} is greater than of octahedral Fe^{3+}. The second ferric doublet compares well with octahedral Fe^{3+} reported for serpentine minerals [22] (I.S. = 0.36—0.55, Q.S. = 0.65—1.08 mm s^{-1}). The present parameters do not compare well with those estimated in previous Mossbauer studies of cronstedtite [1,2], which values are also in disagreement with each other, possibly because of the approximate way in which they were measured. A further major difficulty in comparing I.S. values arises from the failure of both previous authors to specify their reference substance [1,2].

Heating cronstedtite in air to 200°C produces little change in the spectrum, the proportion of Fe^{2+} to total Fe^{3+} remaining essentially unchanged but the proportion of tetrahedral Fe^{3+} to octahedral Fe^{3+} diminishing. Further heating in air to 320°C produced a marked change in the spectrum (Fig. 4B) which could now be resolved into two octahedral Fe^{3+} doublets,

TABLE 4

Mossbauer parameters for unheated and heated cronstedtite (Six-line magnetic spectra omitted; isomer shifts quoted with respect to natural iron)

Atmosphere	Temperature (°C)	I.S (mm s^{-1})	Q.S. (mm s^{-1})	Assignment
—	Unheated	1.21	2.23	Fe^{2+}, Oh
		0.23	0.52	Fe^{3+}, Td
		0 69	0.79	Fe^{3+}, Oh
Air	200	1 23	2.10	Fe^{2+}, Oh
		0 34	0.50	Fe^{3+} Td
		0 76	0 62	Fe^{3+} Oh
	320— 410	1.03—1 39	1.80—2.37	Fe^{2+} Oh
		0 42—0.50	1.30—1.48	Fe^{3+} Oh, distorted
		0 47—0.51	0.70—0.80	Fe^{3+}, Oh
	510— 700	0.44—0 47	1.28—1 51	Fe^{3+}, Oh, distorted
		0.44—0.48	0 71—0.85	Fe^{3+}, Oh
H_2/N_2	200	1.28	2 12	Fe^{2+} Oh
		0.37	0 55	Fe^{3+} Td
		0.83	0.61	Fe^{3+} Oh
	430— 530	1.23—1 35	1.75—1.78	Fe^{2+} Oh
		0.51—0.69	1.32—1.40	Fe^{3+} Oh, distorted
		0.47—0.63	0.75—0.80	Fe^{3+} Oh
	700—1200 (only at 700)	1.17—1.24	2.73—2.81	Fe^{2+}, Fayalite
		0.50	0 87	Fe^{3+} Oh

one of which has parameters similar to the original octahedral Fe^{3+} sites. The other doublet has a similar I.S. value but a much larger quadrupole splitting (1.30 mm s^{-1}), indicating greater distortion in these sites. Ferric peaks with similarly large Q.S. values have been reported in other hydrous iron silicates after oxidation; a ferric peak in oxybiotite with parameters I.S. = 0.37 (re-calculated with reference to natural iron) and Q.S. = 1.34 mm s^{-1} has been explained in terms of "covalence anisotropy" [23a,b] in which the destruction of the hydroxyl environment during oxidation of Fe^{2+} to Fe^{3+} causes the resulting ferric ions to acquire an oxygen environment while still retaining the layer structure of the parent phase. This results in marked differences in the octahedral Fe(III)—O bond lengths and gives rise to anomalously high values of the electric field gradient acting on the Fe^{3+} nucleii, thus producing large quadrupole splittings in these sites [23a,b]. On this basis, the Fe^{3+} doublets with large Q.S. values can be identified as arising from oxidised octahedral Fe^{2+}. By contrast with the previously reported results for oxybiotite [23a,b] no progressive increase in the Q.S. values for this doublet was observed on heating to higher temperatures, suggesting that the essential characteristics of the oxidised phase are established rather more rapidly and at lower temperatures than in the biotite example. No tetrahedral Fe^{3+} could be distinguished in these spectra but a small, diminishing ferrous doublet persisted up to ~410°C. By 510°C, a trace of hematite had

appeared (Fig. 4C) and the occupancy of the more distorted Fe^{3+} sites had markedly increased. A similar spectrum, with larger hematite peaks, was observed in samples heated to 700°C, but by 1000°C the Fe^{3+} doublets had disappeared, leaving only a hematite spectrum (Fig. 4D). The salient points emerging from the Mossbauer spectra in air are therefore:

(i) oxidation sets in between 200 and 320°C, the oxidised form containing a small but diminishing amount of Fe^{2+};

(ii) the oxidised Fe^{2+} continues to reside as Fe^{3+} in distorted octahedral sites but the tetrahedral Fe^{3+} is lost in the earliest stage of oxidation;

(iii) at ~500°C the occupation of the more disordered octahedral Fe^{3+} sites has increased and a trace of hematite appears;

(iv) between 700 and 1000°C the material associated with the original iron sites (i.e. the silicate phase) is completely converted to hematite.

The Mossbauer spectra of samples heated under reducing conditions up to 530°C (Fig. 5A and B) are very similar to those of oxidised samples (Table 4), indicating a similar initial oxidation of Fe^{2+} and the appearance of Fe^{3+} in distorted sites. Figure 6 shows the ratios of Fe^{2+} to total Fe^{3+} plotted as a function of temperature for samples fired both in air and H_2/N_2, from which it is seen that although the proportion of Fe^{2+} decreases under H_2/N_2 during the low-temperature stage, reduction becomes significant at ~400°C, increasing rapidly at 500—700°C with the formation of olivine, the Fe^{2+} parameters of which are quite different from those of the original material. Further reduction leads to an increase in the intensity of the six-line spectrum of metallic iron at the expense of the olivine (Fig. 5D).

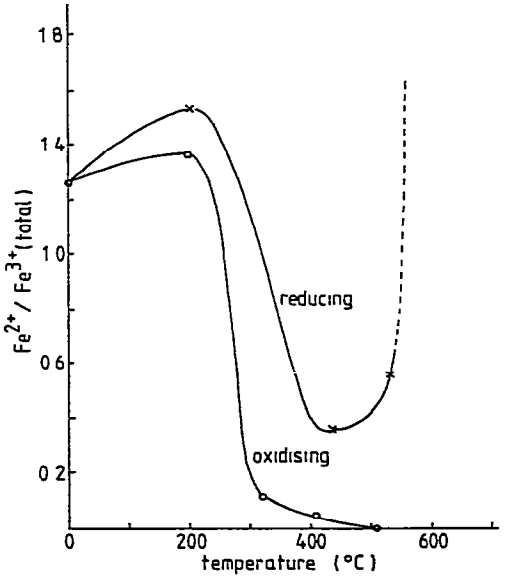

Fig. 6. Mossbauer ratio Fe^{2+}/Fe^{3+} (total) as a function of temperature in oxidising and reducing conditions.

CONCLUSIONS

The thermal reactions occurring in disordered polycrystalline cronstedtite under oxidising and reducing conditions can be summarised as follows.

<200° C. Mechanically-held water is lost, the lattice expands slightly in the *c*-direction and the proportion of tetrahedral Fe^{3+} diminishes.

200—400° C. Hydroxyl water is lost by a mechanism involving internal oxidation of octahedral Fe^{2+}, the resulting octahedral ferric sites being highly distorted. The oxycronstedtite thus formed retains the cronstedtite X-ray pattern but the IR spectrum is broadened and the fine structure is lost. In air, the formation of oxycronstedtite is accompanied by a shrinkage of the lattice which is not, however, observed under reducing conditions.

400—500° C. Further hydroxyl water is lost, accompanied by a progressive loss of the cronstedtite X-ray pattern which is replaced under oxidising conditions by a hexagonal phase, or, under reducing conditions, by a cubic phase. The IR and Mossbauer spectra of these phases are fairly similar, and indicate an intimate association of the silicate with iron, which remains in increasingly distorted octahedral sites. The characteristic six-line hematite Mossbauer spectrum is not observed in the air-fired samples, i.e. at this stage these phases do not represent a mixture of the discrete oxides as suggested by Babcan [6].

>500° C. The iron silicate phase is progressively replaced by hematite (in air) or fayalite (in H_2/N_2). Further reduction of the latter produces metallic iron, with the separation of cristobalite. All these results strongly suggest a degree of structural continuity throughout the reaction.

ACKNOWLEDGEMENTS

We are indebted to Dr. P.E. Desautels, Smithsonian Institution, Washington, for providing the cronstedtite sample, to Mr. A. Cody for the chemical analyses, Dr. D.M. Bibby and Dr. N.B. Milestone for assistance with the thermal analysis, and to Dr. K.L. Brown for assistance with the X-ray crystallography. The Mossbauer curve-fitting programme was written by Dr. L.P. Aldridge.

REFERENCES

1 C E Weaver, J M. Wampler and T.E. Pecuil, Science, 156 (1967) 504.
2 G.L. Taylor, A.P. Ruotsala and R.O. Keeling, Clays Clay Miner., 16 (1968) 381.
3 R. Steadman and P.M. Nuttall, Acta Crystallogr., 16 (1963) 1; 17 (1964) 404.
4 R. Steadman and R.F. Youell, Nature (London), 180 (1957) 1066.
5 R. Steadman and M. Toy, Z. Kristallogr., 122 (1965) 21.
6 J. Babcan, Silikaty, 3 (1960) 20; 6 (1962) 335.
7 S.B. Hendricks, Am. Mineral., 24 (1939) 529.
8 K J.D. MacKenzie and R.M. Beresowski, Thermochim. Acta, 41 (1980) 335.
9 R.C. MacKenzie (Ed.), The Differential Thermal Investigation of Clays, Mineralogical Society Monograph, London, 1957, p. 222

10 (a) W.E. Addison and J.H. Sharp, Clay Miner. Bull., 5 (1962) 73.
(b) W.E. Addison and J.H. Sharp, Clays Clay Miner., 11 (1963) 95.
11 P.G. Rouxhet, J.L. Gillard and J.J. Fripiat, Mineral. Mag., 38 (1972) 583.
12 N.H. Brett, K.J.D. MacKenzie and J.H. Sharp, Q. Rev. Chem. Soc. London, 24 (1970) 185.
13 L. Walter-Levy and E. Quemeneur, Bull. Soc. Chim. Fr., (1968) 495.
14 A. Navrotsky and O.J. Kleppa, J. Inorg. Nucl. Chem., 29 (1967) 2701.
15 H.W. Van der Marel and H. Beutelspacher, Atlas of Infrared Spectroscopy of Clay Minerals and their Admixtures, Elsevier, Amsterdam, 1976, p. 108.
16 (a) C J. Serna, B.D. Velde and J.L. White, Am. Mineral., 62 (1977) 296.
(b) C.J. Serna, J.L. White and B.D. Velde, Mineral. Mag., 43 (1979) 141.
17 V.C. Farmer (Ed.), The Infrared Spectra of Minerals, Mineralogical Society Monograph, London, 1974, Chap. 15.
18 V. Stubican and R. Roy, J Am Ceram. Soc., 44 (1961) 625.
19 V. Stubican and R. Roy, Am. Mineral., 46 (1961) 32
20 M.E. Striefler, G.R. Barsch and Syun-Iti Akimoto, Spectrochim. Acta, Part A, 36 (1980) 275.
21 J. Zussman (Ed.), Physical Methods in Determinative Mineralogy, Academic Press, London, 1977, 2nd edn., p. 555.
22 I. Rozenson, E.R. Bauminger and L. Heller-Kallai, Am. Mineral., 64 (1979) 893.
23 (a) T.S Gendler, L.G. Dainyak and R.N. Kuzmin, Geochem Int., 15 (1978) 17.
(b) V.I. Bagin, T S Gendler, L.G. Dainyak and R.N Kuzmin, Clays Clay Miner., 28 (1980) 188.